Naunyn-Schmiedeberg's Archives of Pharmacology (2021) 394:967–980
https://doi.org/10.1007/s00210-020-02030-w

ORIGINAL ARTICLE

Isoliquiritigenin, an active ingredient of Glycyrrhiza, elicits antinociceptive effects via inhibition of Na_v channels

Yuichi Miyamura[1,2] · Suzuro Hitomi[1] · Yuji Omiya[3] · Izumi Ujihara[1] · Shoichiro Kokabu[4] · Yasuhiro Morimoto[2] · Kentaro Ono[1]

Received: 31 July 2020 / Accepted: 18 November 2020 / Published online: 6 January 2021

Abstract

Glycyrrhiza extract has been used for the treatment of oral and gastric ulcers, but the analgesic mechanism remains unknown. In the present study, we investigated the effects of isoliquiritigenin, an active ingredient of Glycyrrhiza, on Na_v channels in vitro and nociceptive behaviors in vivo. In an autopatch-clamp study, isoliquiritigenin inhibited the currents of $Na_v1.1$, $Na_v1.3$, $Na_v1.6$, $Na_v1.7$, and $Na_v1.8$ in a channel expression system. In small- and medium-sized cultured trigeminal ganglion neurons, the compound suppressed Na_v currents in many neurons (78%) and K_v currents in all neurons, dose-dependently. In current-clamp mode, isoliquiritigenin blocked action potential generation in many neurons (64%), but it conversely accelerated action potential generation in the remaining neurons. The opposing effects on action potentials were reproduced in a computational simulation of a modified Hodgkin-Huxley-based model, based on the electrophysiological data. In behavioral experiments, local treatment with isoliquiritigenin suppressed nociceptive behaviors in response to oral ulcer development or nociceptive TRP channel agonists in the oral mucosa and hind paw. These results suggest that isoliquiritigenin exerts an analgesic effect predominantly via inhibitory action on Na_v channels on sensory nociceptive fibers. This pharmacological mechanism indicates that isoliquiritigenin is useful for pain relief and provides scientific evidence for Glycyrrhiza at the ingredient level.

Keywords Isoliquiritigenin · Na_v channels · K_v channels · Nociception · NEURON simulation

Abbreviations

CFA	Complete Freund's adjuvant
OUM	Oral ulcerative mucositis
ILG	Isoliquiritigenin
LG	Liquiritigenin
BC	Baicalein
WGN	Wogonin
BBR	Berberine
COP	Coptisine
CHO	Chinese hamster ovary
HEK293	Human embryonic kidney 293
FLIPR	Fluorescence imaging plate reader
Lido	Lidocaine
AITC	Allyl isothiocyanate

✉ Kentaro Ono
ono@kyu-dent.ac.jp

Yuichi Miyamura
r16miyamura@fa.kyu-dent.ac.jp

Suzuro Hitomi
hitomi.suzuro@nihon-u.ac.jp

Yuji Omiya
oomiya_yuuji@mail.tsumura.co.jp

Izumi Ujihara
r17ujihara@yahoo.co.jp

Shoichiro Kokabu
r14kokabu@fa.kyu-dent.ac.jp

Yasuhiro Morimoto
rad-mori@kyu-dent.ac.jp

[1] Division of Physiology, Kyushu Dental University, 2-6-1 Manazuru, Kokurakita-ku, Kitakyushu, Fukuoka 803-8580, Japan

[2] Division of Oral and Maxillofacial Radiology, Kyushu Dental University, 2-6-1 Manazuru, Kokurakita-ku, Kitakyushu, Fukuoka 803-8580, Japan

[3] Tsumura Kampo Research Laboratories, Kampo Research & Development Division, Tsumura & Co., 3586 Yoshiwara, Ami-machi, Inashiki-gun, Ibaraki 300-1192, Japan

[4] Division of Molecular Signaling and Biochemistry, Kyushu Dental University, 2-6-1 Manazuru, Kokurakita-ku, Kitakyushu, Fukuoka 803-8580, Japan

TG	Trigeminal ganglion
CPS	Capsaicin
PST	Partial sciatic nerve transection
HOK	Human oral keratinocytes

Introduction

The root of Glycyrrhiza (*Glycyrrhizae Radix*; licorice or liquorice) has been used as a drug for catarrh and wounds and diseases of the stomach, liver, and kidney since ancient Egyptian, Greek, and Roman times (Harding and Stebbing 2017; Shibata 2000). In the East, Glycyrrhiza has also been considered a superior herbal drug since ancient China and is currently one of the most frequently used herbs in traditional Chinese medicine (Shibata 2000; Yang et al. 2015). In modern science, Glycyrrhiza extract was first reported to markedly heal gastric ulcers in many patients (Revers 1956). To date, the extract has been included in an over-the-counter drug used to alleviate stomatitis-induced symptoms (Isbrucker and Burdock 2006). In Japan, the traditional Japanese herbal medicine hangeshashinto, which includes Glycyrrhiza extract, has been clinically used in the treatment of oral ulcerative mucositis (OUM) (Hatakeyama et al. 2015; Kono et al. 2010; Matsuda et al. 2015; Yamashita et al. 2015). Recently, we reported that local treatment with hangeshashinto exerts an analgesic effect on the OUM region in a rat model without any changes in the pain threshold in healthy oral mucosa (Hitomi et al. 2016).

The exploration of active ingredients in therapeutic drugs provides a large contribution to medical science. Some analgesic drugs used in the clinic were originally identified in natural plants with traditionally known analgesic effects, such as morphine in poppy and salicylic acid in willow bark. Hangeshashinto is composed of seven herbal extracts (processed ginger, Glycyrrhiza, scutellaria root, Coptis rhizome, ginseng, jujube, and pinellia tuber). In our previous study, a few ingredients were identified as analgesic compounds in herbal medicine by screening for the effects of 21 major ingredients, as well as the representative analgesic drug lidocaine, on cells expressing the nociception-related $Na_v1.8$ channel. Two phenylpropanoids, [6]-gingerol and [6]-shogaol, from the processed ginger extract showed strong inhibitory effects on $Na_v1.8$ and other subtypes and suppressed OUM-induced pain behaviors (Hitomi et al. 2017).

Isoliquiritigenin (ILG; [*E*]-1-[2,4-dihydroxyphenyl]-3-[4-hydroxyphenyl]prop-2-en-1-one; $C_{15}H_{12}O_4$) is a flavonoid from the Glycyrrhiza extract and is another putative analgesic compound in hangeshashinto because it demonstrated inhibition of $Na_v1.8$ in our previous study (Hitomi et al. 2017). ILG is known to have various pharmacological benefits, including antibacterial and anti-inflammatory effects (Feldman et al. 2011; Kim et al. 2008; Peng et al. 2015). ILG has been reported to inhibit $Na_v1.4$, Ca^{2+} channels, and NMDA receptors (Kawakami et al. 2011; Shi et al. 2012; Zhu et al. 2018), presumably supporting the analgesic effect.

To clarify the ILG-induced analgesic action, we examined the effects of the ingredient on voltage-dependent ion channels in a channel expression system and on the neuronal activities of cultured rat sensory neurons. The reported electrophysiological data were simulated with a modified Hodgkin-Huxley-based model in silico. Finally, we investigated the local effects of ILG on OUM- and drug-inducible nociception and chronic pain status in rats.

Materials and methods

Automated patch-clamp recording

To examine channel specificity of the inhibitory effect of ILG on voltage-dependent channels, ILG was applied to Chinese hamster ovary (CHO) cells expressing one of the following voltage-dependent Na^+ channels: human $Na_v1.1$, $Na_v1.3$, $Na_v1.6$, $Na_v1.7$, and $Na_v1.8$ α-subunits (SCN1A, SCN3A, SCN8A, SCN9A, and SCN10A genes, respectively) with β3-subunits (SCN3B gene), which are expressed in primary nociceptive sensory neurons and involved in inflammatory and neuropathic pain status (Cummins et al. 2007; Tibbs et al. 2016). The experiments were performed at a laboratory company (Charles River Laboratories, Cleveland, OH). Patch-clamp recordings were automatically performed with the QPatch HT system (Sophion Bioscience A/S., Ballerup, Denmark). The intracellular solution contained 120 mM CsF, 30 mM CsCl, 5 mM NaF, 2 mM $MgCl_2$, 10 mM EGTA, and 5 mM HEPES (pH 7.2). The extracellular solution was used for all channels: 137 mM NaCl, 4 mM KCl, 1.8 mM $CaCl_2$, 1 mM $MgCl_2$, 10 mM HEPES, and 10 mM glucose (pH 7.4). Na_v currents were evoked using a stimulus voltage pattern, which consisted of the depolarized test pulse (0 mV for 1 s) following hyperpolarizing conditioning prepulse to − 120 mV for 200 ms from a holding potential of − 80 mV. All evoked Na_v currents were inhibited by the reliable nonselective Na_v channel blocker lidocaine at 2 mM (in 2–3 cells). ILG was applied to 3–4 cells. The concentration of ILG was set to 100 μM, based on the estimated ingredient concentrations in hangeshashinto 100 mg/mL (bioactive dose in previous study [Hitomi et al. 2017]) from proprietary information obtained from Tsumura & Co.

Fluorescence imaging plate reader assay

To investigate the effects of ILG on TRPA1 and $P2X_3$, a Fluo-8 dye Ca^{2+} assay in CHO cells expressing human TRPA1 and in human embryonic kidney 293 (HEK293) cells expressing $P2X_3$ with a fluorescence imaging plate reader (FLIPR)

(FLIPRTETRA™, Molecular Devices) was performed at a laboratory company (ChanTest, Cleveland, OH). In our previous study (Hitomi et al. 2017), the agonistic effects of isoliquiritigenin with the 20 other major ingredients of hangeshashinto, namely, [6]-gingerol, [6]-shogaol, glycyrrhizin, isoliquiritin, liquiritigenin, liquiritin, liquiritin apioside, baicalein, baicalin, wogonin, berberine, coptisine, ferulic acid, palmatine, ginsenoside Rb1, ginsenoside Rg1, betulinic acid, oleanolic acid, corymboside, and homogentisic acid, were investigated. Therefore, these ingredients were also investigated in the present study. Ferulic acid was purchased from Sigma-Aldrich (St. Louis, MO), and all other ingredients were synthesized by Tsumura & Co. Based on the estimated ingredient concentrations in 100 mg/mL hangeshashinto, the concentrations of these ingredients were set to 5 and 50 μM for berberine, coptisine, betulinic acid, and oleanolic acid or 10 and 100 μM for the other ingredients. Dimethyl sulfoxide (DMSO) and Pluronic F-127 were used as vehicles at 0.3% and 0.05%, respectively.

The cells were plated in 384-well microtiter plates with black walls and flat and clear bottoms (BD Biocoat Poly-D-Lysine Multiwell Cell Culture Plates) at 2–3 × 10^4 cells per well and were incubated at 37 °C until the cells attained a sufficient density in the wells (a near-confluent monolayer). In the evaluation of the inhibitory effects of the 21 ingredients, the maximal Ca^{2+} signals induced by the application of channel agonists (TRPA1, allyl isothiocyanate [AITC] at 100 μM; and $P2X_3$, αβ-methylene adenosine triphosphate at 3 μM) were set to 0% inhibition, and those induced by the additional application of a high dose of reliable channel antagonists (TRPA1, ruthenium red at 10 μM; $P2X_3$, PPADS at 100 μM) were set to 100% inhibition. The inhibitory effects are presented as normalized percent inhibition.

Experimental animals

Male Wistar rats (Kyudo, Saga, Japan) were used for all experiments. The rats were housed in pairs in clear cages with wood chips or paper pellets under specific pathogen-free conditions; they were maintained on a light-dark cycle (L:D, 12-h:12-h) in a temperature- and humidity-controlled room (20–26 °C and 30–70%, respectively) with food pellets and water provided ad libitum. All experiments were conducted in accordance with the National Institutes of Health guidelines (Guide for the Care and Use of Laboratory Animals) and the guidelines of the International Association for the Study of Pain to ensure minimal animal use and discomfort (Zimmermann 1983). They were approved by the Animal Experiment Committee of Kyushu Dental University. The rats were randomly selected for each experiment. All behavioral observations were performed with the researcher blinded to the experimental conditions.

Conventional patch-clamp recording from cultured sensory neurons

To examine the effects of ILG on peripheral sensory neurons, we performed conventional patch-clamp recordings from cultured trigeminal ganglion (TG) neurons from rats. Bilateral trigeminal ganglia were quickly removed from 4 to 5-week-old rats under deep anesthesia following the intraperitoneal injection of a mixture of medetomidine (0.375 mg/kg), midazolam (2.0 mg/kg), and butorphanol (2.5 mg/kg) and transferred to Hank's balanced salt solution (Thermo Fisher Scientific). The tissue was incubated in collagenase (2 mg/mL, Wako) and dispase (2 mg/mL, Sankyo, Tokyo, Japan) for 1 h at 37 °C and triturated with a plastic pipette according to a previous study (Zhao et al. 2014). Neurons were further purified using Percoll (GE Healthcare, Pittsburgh, PA) density centrifugation. The cell suspension was washed 3 times with culture medium (Lebovitz-15 medium, Thermo Fisher Scientific) containing 10% fetal calf serum, penicillin, streptomycin, and amphotericin B and then plated onto glass-bottomed dishes coated with poly-D-lysine (MatTek Corp., Ashland, MA). The neurons were cultured for 3–4 days at 37 °C in a humidified chamber prior to the patch-clamp recordings.

Before whole-cell patch-clamp recording, the cultured neurons were superfused with a perfusion solution containing 130 mM NaCl, 5 mM KCl, 1 mM $MgCl_2$, 2 mM $CaCl_2$, 10 mM glucose, and 10 mM HEPES (pH 7.4). Patch pipettes were double-pulled from glass capillaries (GD-15; Narishige, Tokyo, Japan) and adjusted to 2–3 MΩ (for Na_v current recording) or 4–8 MΩ (for other recordings) when filled with the following pipette solutions, according to previous studies (Liang et al. 2013a; Takayama et al. 2015): for Na_v current, 140 mM CsCl, 10 mM NaCl, 0.5 mM $CaCl_2$, 5 mM EGTA, 2 mM ATP-Mg, and 10 mM HEPES (pH 7.4); and for other recordings, 67 mM KCl, 65 mM K-gluconate, 1 mM $MgCl_2$, 5 mM EGTA, 1 mM ATP-Mg, 1 mM GTP-Na_2, and 10 mM HEPES (pH 7.3). Membrane potentials and currents were recorded at room temperature using a patch-clamp amplifier (EPC-8, HEKA Electrinik, Lambrecht, Germany). The series resistance and liquid junction potential in the pipette were not compensated. To isolate Na_v currents, we used a specific extracellular solution, 120 mM NaCl, 5 mM KCl, 30 mM tetraethylammonium Cl, 10 mM 4-amynopyridine, 2 mM $MgCl_2$, 2 mM $CaCl_2$, 0.1 mM $CdCl_2$, 10 mM glucose, and 10 mM HEPES (pH 7.4), according to an early study (Liang et al. 2013a). To isolate K_v current, we used another specific extracellular solution, 130 mM Choline-Cl, 5 mM KCl, 1 mM $MgCl_2$, 2 mM $CaCl_2$, 0.1 mM $CdCl_2$, 10 mM glucose, and 10 mM HEPES (pH 7.4). ILG at 10, 30, 100, and 300 μM (vehicle: 0.1% DMSO as control) in the Na_v and K_v current-specific extracellular solutions were applied to a neuron by a fast-step SF-77B superfusion system (Warner Instrument,

Hamden, CT) with a three-barreled pipette placed near the neuron. Only cells with diameters < 38 μm (small- and medium-sized neurons) were analyzed because they are predominantly related to nociception.

To examine effects of ILG on Na_v and K_v currents, a voltage step to 0 mV (60- and 200-ms duration, respectively) was applied after a 700-ms conditioning pulse to − 100 mV from − 60 mV (9 and 6 neurons, respectively). In Na_v current recording, a series of depolarizing command steps (10-mV steps, 60-ms duration, 1-s interval) was further applied to a final potential of + 20 mV after the same conditioning pulse during application of vehicle and ILG at 100 μM. In current-clamp mode, current steps (0.2-nA steps to a final current of 1.0 nA, 100-ms duration) were applied to the recording neurons before, during, and after (following washout) the drug application to generate action potentials (25 neurons). In some neurons that showed good recovery after drug washout in current-clamp mode (10 neurons), the drug effect on the whole-cell current was additionally investigated in voltage-clamp mode. The whole-cell current was generated by a pulse protocol of 20-mV steps (200-ms duration) from − 60 to 20 mV after a 500-ms conditioning pulse to − 100 mV.

Computational simulation of neuronal activity

To confirm the results from cultured sensory neurons in whole-cell patch-clamp recording, we performed a simulation with NEURON software (version 7.5) (Hines and Carnevale 1997) running under Windows 10. Based on the mean values of the recorded neurons, an isopotential cylinder with a 26-μm diameter (mean cell diameter) with a 13-μm length (hemisphere) and a 0.223-mS/cm^2 leak conductance was used to model a sensory neuron. The intracellular and extracellular concentrations of Na^+ and K^+ were set to the same parameters as in the real experiments (see "Conventional patch-clamp recording from cultured sensory neurons"). The temperature was set to 25 °C. According to a previous study that modeled sensory neurons (Kovalsky et al. 2009), the membrane capacitance and reversal potential of the leak current were set to 1 μF/cm^2 and − 65.5 mV, respectively. As representative Na_v and K_v channels, we used built-in channel membrane mechanisms, Hodgkin-Huxley channels (Hodgkin and Huxley 1952), and a previously created A-type K_v channel (Fineberg et al. 2012). The ion conductances of Na_v (gnabar_hh), sustained K_v (gkbar_hh), and A-type K_v (gmax_kv4csiosi) channels were initially set at 0.0130, 0.08, and 0.005, respectively, as controls, and these values were changed to 0.0013, 0.001, and 0.000, respectively, to simulate the addition of ILG to the neuron. Current and voltage traces were obtained by the same voltage and current step protocols, respectively, used in the whole-cell patch-clamp recordings.

Pain model establishment

OUM model rats were prepared according to our previous study (Hitomi et al. 2015, 2016, 2017; Nodai et al. 2018; Yamaguchi et al. 2016). Under anesthesia with a mixture of intraperitoneally administered medetomidine, midazolam, and butorphanol, the rats were treated at the labial fornix region of the inferior incisors with 50% acetic acid soaked in filter paper (3 mm × 3 mm, Whatman, Maidstone, UK) for 30 s (n = 42). Drug application and pain-related behavioral observations were performed on day 2, and visually apparent ulceration in the treated oral mucosal region was observed.

To acutely evoke nociceptive TRP channel-induced nociception, 100 μL of 1% DMSO-containing saline solution containing the TRPV1 agonist capsaicin (CPS) at 100 μM and the TRPA1 agonist AITC at 10 mM were subcutaneously injected into the hind paw in conscious, using a 31G needle with a 1-mL syringe (n = 39).

As a chronic inflammatory pain model, 8 rats were prepared with an intraplantar injection of emulsified complete Freund's adjuvant (CFA) with the same volume of saline (35 μL) into the right or left hind paw under 2% isoflurane anesthesia (Du et al. 2003). A pain test by von Frey filaments was performed before and 2 days after CFA injection. As a neuropathic pain model, 8 rats were prepared by partial sciatic nerve transection (PST) under anesthesia with a mixture of medetomidine, midazolam, and butorphanol. The exposed sciatic nerve at the left mid-thigh was perforated mid-diameter, and the lateral part was cut by a 31G needle (Lindenlaub and Sommer 2000). A pain test by von Frey filaments was performed before and 1, 3, and 7 days after the PST.

ILG treatments

To examine whether ILG has an algesic effect on oral mucosa, 1% DMSO in distilled water without (control) or with ILG was topically applied to the labial fornix region of the inferior incisors in conscious healthy and OUM model rats (each group, n = 6) with a handheld plastic dropper (VECTASTAIN ABC kit; VectorLab, Burlingame, CA) using an intraoral dropping method (Hitomi et al. 2015, 2016, 2017; Ito et al. 2017; Nodai et al. 2018; Yamaguchi et al. 2016). With the same protocol, 100 μM CPS in 0.1% DMSO in distilled water and 100 mM AITC in mineral oil were applied to examine the analgesic effect of ILG on chemically induced nociception in OUM model rats (n = 12). Under 2% isoflurane anesthesia, 20 μL of a solution with or without ILG was applied to the labial fornix region of the inferior incisors for 5 min (n = 12) using a soaked cotton swab with a diameter of 2 mm (swab application), the same procedure used in our previous studies (Hitomi et al. 2015, 2016, 2017; Ito et al. 2017; Nodai et al. 2018; Yamaguchi et al. 2016). To measure the mechanical threshold, the swab application was

performed on conscious animals ($n = 8$) because these rats were previously trained to stably expose the OUM area while conscious (see "Pain-related behavioral observations").

To examine whether ILG has an algesic effect on the hind paw, 1% DMSO in saline with or without ILG was subcutaneously injected into the hind paw ($n = 14$). To evaluate the analgesic effect of ILG on chemical-induced nociception in the hind paw, 200 μM ILG was subcutaneously coinjected with CPS or AITC (each group, $n = 8$). In the chronic inflammatory and neuropathic pain models, ILG or vehicle (control; 1% DMSO in saline) was subcutaneously injected into the hind paw according to the same protocol (each group, $n = 4$).

Pain-related behavioral observations

For OUM model rats, spontaneous mouth rubbing behavior using both forelimbs was recorded as a sign of spontaneous orofacial pain in a clear plastic cage (30 × 30 × 30 cm) for 10 min at 60 min after drug application. Similarly, the same behavior was measured in the same plastic cage for 3 min (or 5 min when AITC was used) immediately after intraoral dropping, as a chemically induced nociceptive behavior. All rats were acclimated to the clear plastic cage at least three times prior to the behavioral measurements. To measure the head withdrawal mechanical threshold in the oral mucosa of conscious rats, the stable intraoral opening method was performed in a handmade black box (6 × 6 × 13 cm) constructed from a plastic rectangular bottle using a set of von Frey filaments (0.02–0.6 g, North Coast Medical, Morgan Hill, CA) and 0.2- and 0.3-g handmade filaments according to our previous studies (Hitomi et al. 2015, 2016, 2017; Ito et al. 2017; Nodai et al. 2018; Yamaguchi et al. 2016). To expose the oral mucosa, the mental skin of 5-week-old rats under pentobarbital anesthesia (50 mg/kg, intraperitoneal) was pierced with a magnetized ring (22-gauge-like size, Daiso Sangyo, Hiroshima, Japan). The rats were subsequently trained to stably expose the labial fornix region while conscious by attaching a small neodymium magnet with a 4-g weight to the pierced ring for 2–3 weeks prior to the measurements. The mechanical thresholds of the oral mucosa and the hind paw were defined as the minimum pressure required to evoke an escape attempt in at least 3 of the 5 tests.

To measure behaviors related to pain in the hind paw, all rats were acclimated in a clear plastic cage (19 × 21 × 15 cm) on wire-netting for 30 min before testing (one paw per animal as a single N). Immediately after the subcutaneous injection of TRP channel agonists, nociceptive behaviors (licking and flinching of the injected paw and elevating the paw) were measured as a sign of chemically induced pain for 10 min. Paw withdrawal mechanical threshold in conscious rats was measured through the wire-netting, using a set of von Frey filaments (4–60 g, North Coast Medical), based on same criteria for head withdrawal threshold.

Quantification of bacterial counts in OUM

Under anesthesia with a mixture of medetomidine, midazolam, and butorphanol, the mucosal tissue with the most severe mucositis was extracted 1 h after the swab application of ILG ($n = 5$) or vehicle (1% DMSO in distilled water, $n = 5$). According to our previous studies (Hitomi et al. 2017; Ito et al. 2017; Nodai et al. 2018; Yamaguchi et al. 2016), the mucosal tissue was placed in a pre-weighted 1.5-mL plastic tube filled with 0.5 mL of sterilized phosphate-buffered saline, and the sample was ultra-sonicated for 30 s (38 kHz, US-2; SND Co., Nagano, Japan) to leach out the oral bacteria. Each sample was adequately diluted, and 50-μL sample aliquots were plated in duplicate onto brain-heart infusion agar (Nissui Co., Tokyo, Japan). After an overnight incubation at 37 °C in aerobic conditions, the colony-forming units of the culture plates were manually counted.

Cytotoxicity test in human oral keratinocytes

ILG has been reported to have cytotoxicity at concentrations over 100 μM after 24 h of treatment (Na et al. 2018). To confirm the cytotoxicity of the short-term use of 100 and 200 μM ILG, a cytotoxicity assay in oral keratinocytes was performed using a Cell Counting Kit-8 (Dojindo, Kumamoto, Japan). According to previous studies (Hitomi et al. 2017; Kono et al. 2014), human oral keratinocytes (HOK, Lot No. 5854; ScienCell Research Laboratories, Carlsbad, CA, passage 3) were maintained in poly-L-lysine-coated dishes in keratinocyte-SFM medium (Thermo Fisher Scientific) containing epidermal growth factor (50 μg/mL), bovine pituitary extract (5 μg/mL), 10% fetal calf serum, penicillin, and streptomycin at 37 °C in a humidified 5% CO_2 chamber. The HOK cells were seeded in 96-well plates at a density of 5000 cells per well and incubated with 100 or 200 μM ILG or the control condition (0.1% DMSO) for 2 h. According to the recommendations of the manufacturer of the Cell Counting Kit-8, the cell viability after drug treatment was calculated as the percentage of absorbance (450 nm) relative to the control.

Statistical analysis

The data are presented as the mean ± standard error of the mean (SEM). In the FLIPR assay, the inhibitory effects were considered significant if the mean value was three or more standard deviations (SDs) different from the vehicle. Unpaired and paired Student's t tests were used to compare the differences between two different treatments or days. Sidak's post hoc test following two-way repeated measures analysis of variance (ANOVA) was used to analyze the time changes between two different groups. Sidak's or Dunnett's post hoc test following one-way repeated measures ANOVA was used to analyze nociceptive behaviors and the effect of day on changes in the

mechanical threshold of the neuropathic pain model. A Mann-Whitney *U*-test was used to compare between-group differences in the number of bacterial colony-forming units. The conductance of pharmacologically isolated Na_v current was calculated using the equilibrium potential of Na^+ (+ 64 mV) and normalized by the maximal conductance. The relationships between normalized conductance and membrane potential were fitted by the Boltzmann equation. The best-fit values of V_{50} or slope between control and ILG application were compared by extra sum-of-squares F test. Differences were considered significant at P values < 0.05.

Results

Effects of ILG on nociception-related Na_v channels

To examine the specificity of ILG to Na_v channel α-subunits, the effects of ILG at 100 μM were systematically investigated with automated patch-clamp recordings of CHO cells expressing human $Na_v1.1$, $Na_v1.3$, $Na_v1.6$, $Na_v1.7$, and $Na_v1.8$. ILG exhibited nonselective inhibitory effects on the evoked inward currents generated by these Na_v channels, as well as the representative local anesthetic drug lidocaine at 2 mM (Fig. 1a, b).

Effects of ILG on TRPA1 and $P2X_3$ channels

In our previous study (Hitomi et al. 2017), ILG was reported to activate human TRPV1 and TRPA1 in a FLIPR assay, although the efficacy was weak (a few percent of CPS-induced and approximately 20% of AITC-induced Ca^{2+} responses, respectively). ILG exhibited a strong inhibitory effect on human TRPA1 (Fig. 1c), probably due to desensitization following the agonistic effects on the channel. In a FLIPR assay investigating the inhibitory effects on human $P2X_3$, ILG exhibited an inhibitory effect on the nociceptive channel (Fig. 1d). Together with ILG, we performed the same analyses with the other 20 ingredients of hangeshashinto, similar to our previous study (Hitomi et al. 2017). Figure 1 c and d show the numerical data of 8 ingredients that demonstrated some effects on channels in the previous study. The remaining 13 ingredients did not show any effects on TRPA1 (Supplementary Table 1). [6]-Shogaol and liquiritigenin exhibited significant strong and weak inhibitory effects on TRPA1, respectively (Fig. 1c). In our previous study, [6]-shogaol exhibited a strong agonistic effect on this channel (Hitomi et al. 2017). [6]-Gingerol, [6]-shogaol, liquiritigenin, and baicalein exhibited significant inhibitory effects on human $P2X_3$ (Fig. 1d). Additionally, glycyrrhizin, isoliquiritin, liquiritin, and baicalin have weak inhibitory effects on $P2X_3$ (Supplementary Table 1).

Effects of ILG on Na_v current and action potential generation in cultured sensory neurons

To pharmacologically isolate whole Na_v current in cultured sensory neurons from rats, we used K_v and Ca_v channel blocker-containing extracellular solution and relatively low resistance pipettes filled with a Cs-based internal solution. Because there was no compensation for series resistance, the given current traces in the voltage-clamp mode were slightly distorted from previously reported Na_v current kinetics (Fig. 2a). ILG at 10–300 μM was applied to a recording neuron after application of vehicle (control, 0.1% DMSO-containing extracellular solution). In 7 of 9 neurons, ILG inhibited the Na_v currents that were generated by a voltage step of 0 mV, dose-dependently (Fig. 2a), but did not in 2 other neurons (slightly increases to 109 and 118% at 100 μM). To examine effect of ILG on the voltage dependence of current activation, we applied a series of voltage steps with 10-mV increment from − 70 mV to a final step to + 20 mV to the same 9 neurons during application of vehicle and ILG at 100 μM. Figure 2b shows activation curves of Na^+ conductance in the absence and presence of ILG at 100 μM. ILG was significantly reduced Na^+ conductance over − 20 mV ($P < 0.01$ in Sidak's post hoc test following a two-way ANOVA). The voltage dependence was significantly shifted to the right following ILG application (V_{50}: from − 20.5 ± 1.4 mV to − 12.2 ± 1.5 mV; $P < 0.01$ in F test) without any change of slope values (control, 5.4 ± 1.3 mV and ILG, 4.0 ± 1.3 mV).

In 25 cultured sensory neurons, we investigated the effects of ILG on current injection-induced action potentials in current-clamp mode. The mean cell diameter was 26.4 ± 0.8 μm, and the leak conductance was 5.3 ± 1.2 pS. The resting membrane potential was − 54.1 ± 3.2 mV, and no neurons showed spontaneous firing. In 7 neurons (28%), ILG at 100 μM depolarized membrane potential (14.0 ± 2.8 mV). Importantly, in 16 neurons (64%), the application of ILG at 100 μM blocked action potential generation during current injection (current threshold before ILG application: 0.36 ± 0.04 nA), even under ILG-induced depolarization (Fig. 2c). However, in the remaining 9 neurons, ILG decreased the current threshold (0.69 ± 0.07 nA to 0.20 ± 0.00 nA, $P < 0.01$ in Student's t test) and prolonged action potential (Fig. 2d), indicating an excitatory effect. There was a significant difference in the current threshold before ILG application between neuron groups that showed inhibitory and excitatory actions ($P < 0.01$, in Student's t test). A high dose (300 μM) of ILG also demonstrated similar opposing effects in 3 neurons (inhibitory, $n = 2$ and excitatory, $n = 1$).

The inhibitory and excitatory effects of ILG on action potential generation were reversible 3–5 min after washing out the drugs (Fig. 2c, d). Therefore, in each 5 neurons in both groups, whole-cell currents were further recorded in voltage-clamp

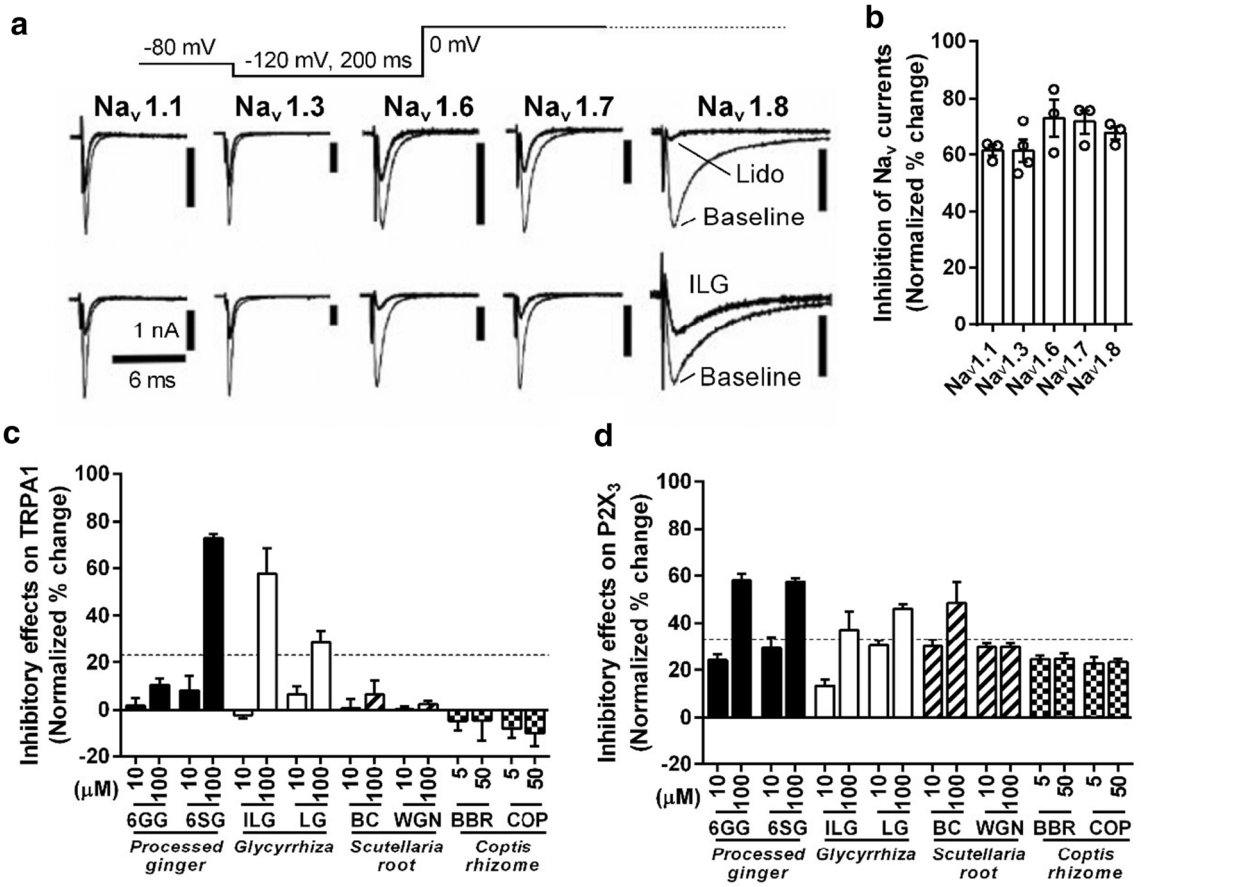

Fig. 1 Inhibitory effects of isoliquiritigenin (ILG) on human Na_v, TRPA1, and $P2X_3$ channels in a channel expression system. **a** Superimposed traces of Na_v currents at baseline and after the applications of the representative Na_v blocker lidocaine (Lido) at 2 mM and ILG at 100 μM. Thin and thick lines represent the baseline and drug application traces, respectively. **b** Inhibitory effects of ILG on the Na_v currents (3–4 cells). Percent change indicates a percentage of inhibited current component against full current. **c**, **d** Inhibitory effects of the ingredients on TRPA1 and $P2X_3$, respectively, in FRIPR assay. 6GG, [6]-gingerol; 6SG, [6]-shogaol; ILG, isoliquiritigenin; LG, liquiritigenin; BC, baicalein; WGN, wogonin; BBR, berberine; COP, coptisine. This figure represents only the 8 hangeshashinto ingredients that demonstrated some effects on channels in our previous study (Hitomi et al. 2017). Four replicated wells/concentrations were used for each experiment. Dashed lines indicate three SDs greater than the vehicle application. Effects were considered significant if the mean value was greater than the dashed lines. Because given FLIPR data from ChanTest was mean ± SD, the graphs are shown only bars without data plots

mode. During ILG application, fast inward component, presumed to Na_v current, was largely diminished in all neurons that showed inhibitory action (Fig. 2c), but they were still remained in all neurons that showed excitatory action (Fig. 2d). Additionally, outward component, presumed to K_v current, was diminished in both groups by ILG application (Fig. 2c, d).

Computational simulation of ILG effects

We investigated effect of ILG on pharmacologically isolated K_v currents, by using Ca_v channel blocker-containing Na^+-free extracellular solution. In all tested 6 neurons, ILG suppressed sustained current component of the isolated K_v currents, dose-dependently (Fig. 3a; inhibitory effects: 7.3 ± 2.4, 16.8 ± 10.1, 51.3 ± 5.1, and 74.5 ± 6.0% at 10, 30, 100, and 300 μM, respectively). In 4 of the 6 neurons, A-type current component (transient) was detected with sustained K_v currents and also suppressed by ILG. After washout of ILG, the isolated K_v currents were recovered to a some degree and blocked by the general K_v channel blockers, tetraethylammonium at 30 mM and 4-amynopyridine at 10 mM ($n = 3$; Fig. 3a).

By usage of given results in Na_v and K_v currents, we performed computational simulation in a neuron model using NEURON software. In the neuron model, we included the A-type K_v current (Fineberg et al. 2012) with the Hodgkin-Huxley model, which consists of a fast active Na_v current and a sustained K_v current that resembles the real whole-cell current in cultured sensory neurons (left traces on the bottom of Fig. 2c, d and the top of Fig. 3b). Each ion conductance parameter was set to generate an action potential from a 0.4-nA current injection (left traces on the bottom of Fig. 3b). The strong inhibition of both inward and outward currents that mimicked the inhibitory action of ILG decreased the action potential generation following 0.4- and 0.6-nA current

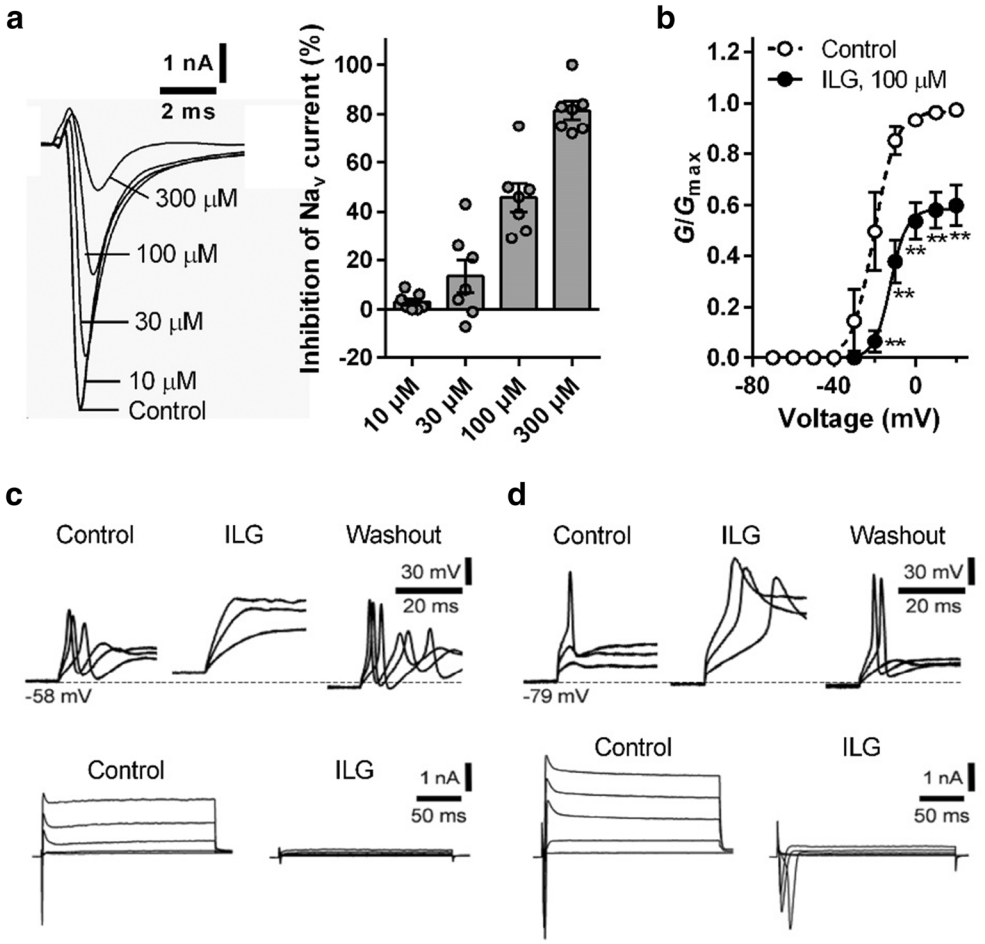

Fig. 2 Inhibitory effects of isoliquiritigenin (ILG) on Na_v currents in cultured trigeminal ganglion neurons from rats. **a** Dose dependence of inhibitory effects of ILG on pharmacologically isolated Na_v currents by a voltage step to 0 mV after a 700-ms conditioning pulse to − 100 mV from − 60 mV of holding potential ($n = 7/9$). Current trace is a representative Na_v current following ILG application. **b** Na^+ conductance (G) normalized by the maximal conductance (G_{max}) in control and 100 μM ILG application ($n = 7$). ** indicates $P < 0.01$ in Sidak's post hoc test following two-way ANOVA. **c** Representative traces of the changes in voltage and current before (control), during (ILG) and after (washout) the application of ILG at 100 μM in neurons showing inhibitory action (voltage: $n = 16/25$, 64% and current: $n = 5$). Top traces represent the changes in voltage that occurred in the response to current steps (0.2, 0.4, and 0.6 nA). Bottom traces represent the changes in current that occurred in response to voltage steps (from − 60 to 20 mV at 20 mV increments, following a prepulse of − 100 mV for 500 ms). **d** Representative traces of the changes in voltage and current before (control), during (ILG), and after (washout) application of ILG in neurons showing excitatory action (voltage: $n = 9/25$, 36% and current: $n = 5$)

injection in the current-clamp simulation (middle traces in Fig. 3b). The strong inhibition of only outward currents that mimicked the excitatory action of ILG generated a broad action potential in response to a low current injection (0.2 nA) (right traces in Fig. 3b). These simulation results closely matched the actual results collected from cultured trigeminal ganglion neurons (Fig. 2c, d).

Effects of ILG on OUM-induced pain

Since ILG has a weak agonistic effect on nociceptive TRP channels (Hitomi et al. 2017), we first confirmed whether ILG elicits pungency in the oral mucosa. By using an intraoral dropping method, mouth rubbing behavior (a sign of intraoral pain) was measured for 3 min immediately after the transient application of ILG at 200 μM in healthy normal rats. The concentration administered was twofold that of the estimated content in 100 mg/mL hangeshashinto, which demonstrated an analgesic effect in our previous study (Hitomi et al. 2016, 2017). At that concentration, ILG administration did not prolong the mouth rubbing time in the healthy normal rats compared with the control (each group $n = 6$; Fig. 4a). Similarly, in OUM model rats, ILG at that concentration did not show any effect on mouth rubbing behavior (each group $n = 6$; Fig. 4a).

All OUM model rats were demonstrated to have a reduced mechanical head withdrawal threshold in the OUM region compared with rats with healthy mucosa before acetic acid treatment ($n = 8$, data not shown), consistent with previous studies (Hitomi et al. 2015, 2016, 2017; Nodai et al. 2018; Yamaguchi et al. 2016). Compared with the control, the swab

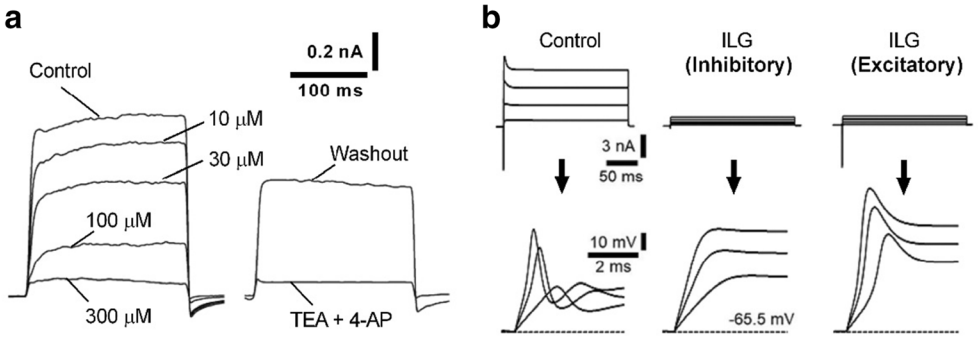

Fig. 3 Effects of isoliquiritigenin (ILG) on K_v currents in cultured trigeminal ganglion neurons from rats and computational simulation of neuronal activity in a Hodgkin-Huxley-based model. **a** Inhibitory effects of ILG on pharmacologically isolated K_v currents by a voltage step to 0 mV after a 700-ms conditioning pulse to − 100 mV from − 60 mV of holding potential ($n = 6$). Current trace in the left side is a representative K_v current following ILG application. After washout of ILG, recovered outward current components were blocked by the general K_v channel blockers, tetraethylammonium at 30 mM and 4-amynopyridine at 10 mM (TEA +4-AP; the right side trace, $n = 3$). **b** Simulation of neuronal activity in a Hodgkin-Huxley-based model combined with the A-type K_v channel under the present real experimental conditions. Current (top) and voltage (bottom) traces were obtained by the same voltage and current step protocols, respectively, used in the whole-cell patch-clamp recordings

application of ILG at 200 μM for 5 min on conscious rats significantly improved mechanical allodynia from 30 and 60 min ($n = 4$, $P < 0.01$ at both time points, Sidak's post hoc test following two-way ANOVA, Fig. 4b). Furthermore, compared with the vehicle treatment, the same ILG treatment significantly suppressed spontaneous mouth rubbing behavior, which is a sign of spontaneous pain, at 1 h after the treatment (each group, $n = 6$; $P < 0.01$, Student's t test; Fig. 4c). Similarly, AITC- and CPS-induced mouth rubbing behaviors, which are signs of chemical hypersensitivity, were also suppressed by the swab treatment of ILG compared with the control condition (each group, $n = 6$; $P < 0.01$ and 0.05 for AITC and CPS, respectively, Student's t test; Fig. 4d, e).

Effects of ILG on the bacterium in the OUM and oral keratinocytes

The swab application of the compound did not change the contents of oral bacteria in the OUM region at 1 h after the treatment relative to vehicle treatment (colony-forming units: ILG, $6.2 \pm 1.3 \times 10^5$ cells/tissue; vehicle, $6.8 \pm 1.4 \times 10^5$ cells/tissue; each group, $n = 5$). Furthermore, ILG at 100 and 200 μM showed no cytotoxicity on human oral keratinocyte cells at 2 h after treatment (cell viability: 100 μM, 114 ± 2% of control; 200 μM, 132 ± 5% of control, 100 ± 4%; each group, 5 wells), suggesting no cytotoxic effects on the oral mucosa.

Effects of ILG in paw pain models

To examine the universal effects of ILG, we measured pain-related behaviors following the subcutaneous injection of ILG or saline (control) into the hind paw, which is the most frequently investigated region in pain research. Compared with the control injection, the subcutaneous injection of ILG at 200 μM into the hind paw did not induce nociceptive behaviors (each group, $n = 7$; Fig. 5a), which corresponded to the action of ILG on the oral mucosa (Fig. 4a). Importantly, compared with the control, the same ILG treatment did not elicit a significant change in the mechanical threshold of the injected paw region (each group, $n = 6$; Fig. 5b).

Therefore, we next examined the analgesic effect of ILG on chemically induced pain in the paw skin. To evoke the painful condition, 100 μM of the TRPV1 agonist CPS and 10 mM of the TRPA1 agonist AITC were subcutaneously injected into the hind paw. Compared with the control injection, the CPS or AITC injection robustly induced nociceptive behaviors (e.g., licking and flinching; each $n = 5$, $P < 0.01$ for CPS and $P < 0.05$ for AITC, Sidak's post hoc test following one-way ANOVA; Fig. 5a). The AITC injection reduced the mechanical threshold ($n = 6$, $P < 0.05$ at 15 and 45 min and $P < 0.01$ at 30 min, Sidak's post hoc test following two-way ANOVA; Fig. 5b). The coinjection of ILG significantly suppressed all these chemically induced nociceptive behaviors (CPS, $n = 6$, $P < 0.01$; AITC, $n = 8$, $P < 0.05$; Sidak's post hoc test following one-way ANOVA; Fig. 5a). The AITC-induced mechanical allodynia were significantly suppressed by coinjection with ILG ($n = 6$, $P < 0.05$ at 15, 30, and 60 min and $P < 0.01$ at 45 min; Sidak's post hoc test following two-way ANOVA; Fig. 5b).

To examine the effects of ILG on chronic pain status, we subcutaneously injected ILG at 200 μM into the hind paw of rat models of chronic inflammatory pain and neuropathic pain. In the chronic inflammatory pain model, the mechanical threshold of paw withdrawal was significantly reduced on day 2 after CFA injection compared with baseline ($n = 8$, $P < 0.01$ in Student's t test, compared with preinjection [baseline]; Fig. 5c). In a chronic neuropathic pain model induced by PST, the mechanical threshold was significantly reduced on day 3, but not on day 2, after the surgery ($n = 8$, $P < 0.01$ on

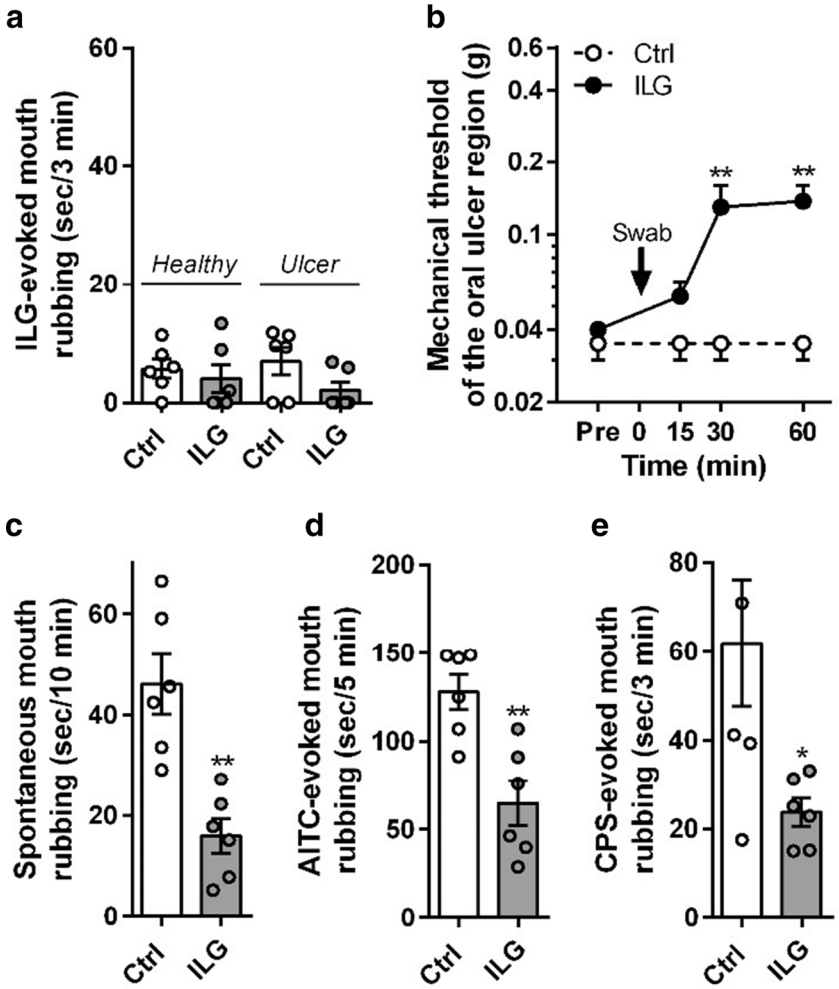

Fig. 4 Effects of isoliquiritigenin (ILG) on pain hypersensitivity in oral ulcerative mucositis (OUM). Control (Ctrl, vehicle) for ILG: 1% DMSO in distilled water. **a** Induced mouth rubbing period immediately after the application of ILG at 200 μM in naïve rats (healthy) and in the OUM model (6 rats per group). **b** Change in the mechanical threshold of head withdrawal after the swab application of Ctrl and ILG (4 rats). $*P < 0.01$ in Sidak's post hoc test following two-way ANOVA, compared with Ctrl. **c** Spontaneous mouth rubbing time 60 min after the swab application of Ctrl and ILG (6 rats per treatment). $**P < 0.01$ in Student's *t* test, compared with Ctrl. **d** The mouth rubbing time induced by the TRPA1 agonist allyl isothiocyanate (AITC)- at 60 min after the swab application of Ctrl and ILG (6 rats per treatment). AITC was diluted to 100 mM in mineral oil. $**P < 0.01$ in Student's *t* test, compared with Ctrl. **e** The mouth rubbing time induced by the TRPV1 agonist capsaicin (CPS)- at 60 min after the swab application of Ctrl and ILG (6 rats per treatment). CPS solution (100 μM in 0.1% DMSO in distilled water) was applied on the same day on the same rats after the application of AITC. $*P < 0.05$ in Student's *t* test, compared with Ctrl

day 3 and 7 in Dunnett's post hoc test following one-way ANOVA, compared with presurgery [baseline]; Fig. 5d). Compared with the control, the subcutaneous injection of ILG did not improve the reduced mechanical threshold in the inflammatory pain model on day 2 or the neuropathic pain model on day 7 (Fig. 5c, D).

Discussion

The present study is the first report demonstrating the analgesic effect of local treatment with ILG at the molecular, cellular, and organismal levels. Since ILG had inhibitory effects on Na_v channels, the analgesic effect of the compound seems to be exerted by the effects on these channels in peripheral nociceptive fibers because of the ability to block action potential conduction. In fact, the local treatment of ILG significantly suppressed nociception in OUM model rats and TRP channel agonist-injected rats. Although the analgesic actions induced by ILG were clearly demonstrated in pain models, the subcutaneous injection of ILG alone into the hind paw did not change withdrawal mechanical threshold, suggesting no anesthetic effect. We found the two contradictive effects of ILG on action potential generation in sensory neurons, due to ILG-resistant Na_v current in a subpopulation. The present computational simulation reproduced the opposing effects on action potential generation, based on electrophysiological observations of Na_v and K_v currents. The absence of an anesthetic

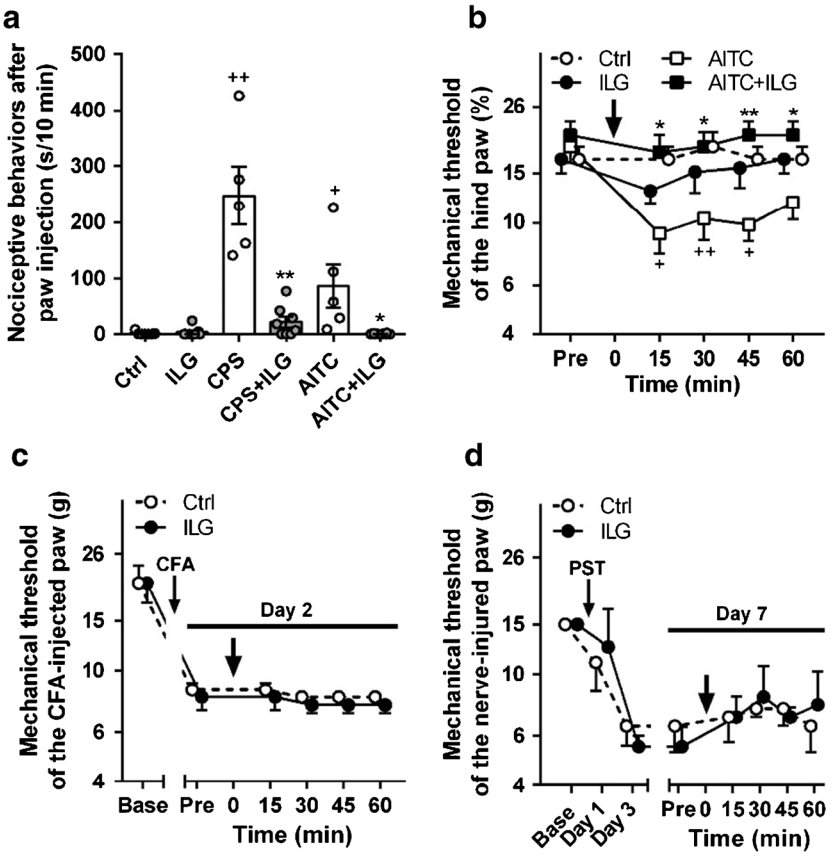

Fig. 5 Effects of isoliquiritigenin (ILG) on nociception in the hind paw. Ctrl, control (vehicle: 1% DMSO in distilled water) for ILG at 200 μM. CPS, the TRPV1 agonist capsaicin at 100 μM; AITC, the TRPA1 agonist allyl isothiocyanate at 10 mM; +ILG, coinjection with ILG; CFA, complete Freund's adjuvant; PST, partial sciatic nerve transection. **a** Induced nociceptive behaviors immediately after the subcutaneous injection of ILG in naïve rats (5–8 rats per group). $^{+}$ and $^{++}$ represent $P < 0.05$ and 0.01, respectively, compared with Ctrl, and * and ** represent $P < 0.05$ and 0.01, respectively, compared with CPS or AITC only, in Sidak's post hoc test following one-way ANOVA. **b** Change in the mechanical threshold after the subcutaneous injection of AITC with or without ILG (each group, 6 rats). $^{+}$ and $^{++}$ represent $P < 0.05$ and 0.01, respectively, compared with Ctrl, and * and ** represent $P < 0.05$ and 0.01, respectively, compared with AITC only, in Sidak's post hoc test following two-way ANOVA. **c** Change in the mechanical threshold after the subcutaneous injection of Ctrl or ILG in an inflammatory pain model injected with CFA (each group, 4 rats). **d** Change in the mechanical threshold after the subcutaneous injection of Ctrl or ILG in a neuropathic pain model induced by PST (each group, 4 rats)

effect of ILG on healthy tissue seems to be caused by masking the inhibitory action in a subpopulation due to excitatory action in the other neuronal subpopulation. ILG is an ingredient of Glycyrrhiza that is one of the longest-used drugs in human history (Peng et al. 2015). This study provides scientific evidence for the analgesic effect of Glycyrrhiza extract at the single ingredient level.

ILG is a chalconoid substituted with three phenolic hydroxyl groups and is classified as a member of the large flavonoid family. In the present study, we revealed novel inhibitory effects of ILG on $Na_v1.1$, $Na_v1.3$, $Na_v1.6$, and $Na_v1.7$ in CHO cells, in addition to $Na_v1.4$ and $Na_v1.8$ as reported in our and other group's previous studies (Hitomi et al. 2017; Zhu et al. 2018). Quick recovery of ILG effects in cultured sensory neurons suggests that ILG seems to be directly combined with these Na_v channels, rather than through regulation of phosphorylation process. A previous study reported that ILG inhibits the sustained K^+ current of $K_v1.5$ in CHO cells and of $K_v2.1$ in H9c2 cells (Noguchi et al. 2008). Some chalcones/flavonoids have been reported to activate TRPA1 at lower doses than the representative agonist AITC (Moriello et al. 2016; Nakamura et al. 2016). These studies further reported that chalcones/flavonoids induce strong desensitization of TRPA1 and that its glycosides lose activity against the channel. The ILG-induced TRPA1 inhibition might partly contribute the analgesic action on AITC-induced nociception. The pharmacological characteristics of ILG against Na_v, K_v, and TRPA1 are likely dependent on the chalcone structure and therefore nonselectively affect various ion channels.

ILG has been reported to exert anti-inflammatory and antibacterial effects (Feldman et al. 2011; Kim et al. 2008; Peng et al. 2015). In our study of OUM model rats, the swab application of reliable antibacterial and anti-inflammatory agents on the OUM region was insufficient to exert these effects 30 min after the treatment (Hitomi et al. 2016). In the present study, the swab application of ILG did not change the oral bacterial contents of the OUM region 1 h after the treatment.

Therefore, we consider the analgesic effects of ILG in the OUM model rats to be simply exerted by the inhibitory actions of ILG on Na_v channels.

Neuropathic pain is defined as pain caused by a lesion or disease of the somatosensory nervous system (International Association for the Study of Pain Home Page 2020). The subcutaneous injection of ILG did not elicit any improvement of mechanical allodynia in the chronic inflammatory and neuropathic pain models. The same results have been observed with the injection of lidocaine in a previous study (Shao et al. 2015). Chronic pain models induced by CFA and PST have been reported to have altered ion channel and receptor expression in primary sensory neurons compared with healthy conditions, the upregulation of $Na_v1.7$, $Na_v1.8$, and TRPV1 (Hudson et al. 2001; Liang et al. 2013b). Recent accumulated evidence indicates that central pain sensitization is chronically caused in some pain models, resulting in the development of morphine-resistant pain and/or ectopic pain (Catheline et al. 2001; Fujita et al. 2019). Therefore, the absence of an analgesic effect of ILG on chronic pain may be due to the low contribution of the primary sensory mechanism to pain perception.

In addition to analgesic effects, ILG and/or Glycyrrhiza extract are known to have various pharmacological benefits for cancer, microbial infection, inflammation, spasm, and so on (Feldman et al. 2011; Kim et al. 2008; Peng et al. 2015; Shi et al. 2012; Takahashi et al. 2004). The extract has already been used as an over-the-counter drug for OUM treatment (Messier et al. 2012; Moghadamnia et al. 2009). ILG is likely to be related to the analgesic effect of the Japanese herbal medicine hangeshashinto that contains Glycyrrhiza extract, in addition to the other two ingredients, [6]-shogaol and [6]-gingerol, reported in our previous study (Hitomi et al. 2017). In cancer patients, chemoradiotherapy causes severe OUM, leading to intractable pain and disruptions in eating, talking, and swallowing. Hangeshashinto has been used in Japan for cancer patients and has reported beneficial effects, including improvements in OUM severity and chemoradiation completion rates (Hatakeyama et al. 2015; Kono et al. 2010; Matsuda et al. 2015; Yamashita et al. 2015). Our findings provide scientific evidence supporting the use of these herbal medicines for OUM-induced pain.

In conclusion, ILG exerts analgesic action via a predominant inhibitory effect on Na_v channels on nociceptive sensory fibers. Identification of ILG-resistant Na_v channel subtypes and molecular mechanism as a gating modifier are needed to investigate in detail as further study.

Supplementary Information The online version contains supplementary material available at https://doi.org/10.1007/s00210-020-02030-w.

Acknowledgments The authors are grateful to Miho Nitta for her technical assistance.

Authors' contribution The first author, Y.M., performed most behavioral experiments and all of the patch-clamp recordings from cultured TG neurons. S.H. prepared the rat OUM model and administered the drugs to ensure that the first author, Y.M., was blinded to the conditions of the behavioral experiments. S.K. prepared the rat neuropathic pain model. Y.O. organized the channel-screening test. I.U. and the sixth author Y.M. designed the experiments and supervised the research. The corresponding author, K.O., designed all experiments and organized the study. All authors have read and approved the manuscript. The authors declare that all data were generated in-house and that no paper mill was used.

Funding This work was funded by Tsumura & Co. (Tokyo, Japan) and a Grant-in-Aid from the Ministry of Education, Culture, Sports, Science and Technology of Japan (JSPS KAKENHI 25861760 and 15K20377). Y.O. is an employee of Tsumura & Co. K.O. and S.H. received grant support from Tsumura & Co.

Compliance with ethical standards

Conflict of interest Y.O is an employee of Tsumura & Co.

Ethical approval All animal experiments were approved by the Animal Experiment Committee of Kyushu Dental University (approval nos. 18-002 and 18-006).

References

Catheline G, Le Guen S, Besson JM (2001) Intravenous morphine does not modify dorsal horn touch-evoked allodynia in the mononeuropathic rat: a Fos study. Pain. 92:389–398. https://doi.org/10.1016/S0304-3959(01)00283-4

Cummins TR, Sheets PL, Waxman SG (2007) The roles of sodium channels in nociception: implications for mechanisms of pain. Pain 131: 243–257. https://doi.org/10.1016/j.pain.2007.07.026

Du J, Zhou S, Coggeshall RE, Carlton SM (2003) N-methyl-D-aspartate-induced excitation and sensitization of normal and inflamed nociceptors. Neuroscience. 118:547–562. https://doi.org/10.1016/S0306-4522(03)00009-5

Feldman M, Santos J, Grenier D (2011) Comparative evaluation of two structurally related flavonoids, isoliquiritigenin and liquiritigenin, for their oral infection therapeutic potential. J Nat Prod 23:1862–1867. https://doi.org/10.1021/np200174h

Fineberg JD, Ritter DM, Covarrubias M (2012) Modeling-independent elucidation of inactivation pathways in recombinant and native A-type Kv channels. J Gen Physiol 140:513–527. https://doi.org/10.1085/jgp.201210869

Fujita S, Yamamoto K, Kobayashi M (2019) Trigeminal nerve transection-induced neuroplastic changes in the somatosensory and insular cortices in a rat ectopic pain model. eNeuro. https://doi.org/10.1523/ENEURO.0462-18.2019

Harding V, Stebbing J (2017) Liquorice: a treatment for all sorts? Lancet Oncol 18:1155. https://doi.org/10.1016/S1470-2045(17)30628-9

Hatakeyama H, Takahashi H, Oridate N, Kuramoto R, Fujiwara K, Homma A, Takeda H, Fukuda S (2015) Hangeshashinto improves the completion rate of chemoradiotherapy and the nutritional status in patients with head and neck cancer. ORL J Otorhinolaryngol Relat Spec 77:100–108. https://doi.org/10.1159/000381026

Hines ML, Carnevale NT (1997) The NEURON simulation environment. Neural Comput 9:1179–1209. https://doi.org/10.1162/neco.1997.9.6.1179

Hitomi S, Ono K, Miyano K, Ota Y, Uezono Y, Matoba M, Kuramitsu S, Yamaguchi K, Matsuo K, Seta Y, Harano N, Inenaga K (2015) Novel methods of applying direct chemical and mechanical stimulation to the oral mucosa for traditional behavioral pain assays in

conscious rats. J Neurosci Methods 15:162–169. https://doi.org/10.1016/j.jneumeth.2014.10.013

Hitomi S, Ono K, Yamaguchi K, Terawaki K, Imai R, Kubota K, Omiya Y, Hattori T, Kase Y, Inenaga K (2016) The traditional Japanese medicine hangeshashinto alleviates oral ulcer-induced pain in a rat model. Arch Oral Biol 66:30–37. https://doi.org/10.1016/j.archoralbio.2016.02.002

Hitomi S, Ono K, Terawaki K, Matsumoto C, Mizuno K, Yamaguchi K, Imai R, Omiya Y, Hattori T, Kase Y, Inenaga K (2017) [6]-gingerol and [6]-shogaol, active ingredients of the traditional Japanese medicine hangeshashinto, relief oral ulcerative mucositis-induced pain via action on Na(+) channels. Pharmacol Res 117:288–302. https://doi.org/10.1016/j.phrs.2016.12.026

Hodgkin AL, Huxley AF (1952) A quantitative description of membrane current and its application to conduction and excitation in nerve. J Physiol 117:500–544. https://doi.org/10.1113/jphysiol.1952.sp004764

Hudson LJ, Bevan S, Wotherspoon G, Gentry C, Fox A, Winter J (2001) VR1 protein expression increases in undamaged DRG neurons after partial nerve injury. Eur J Neurosci 13:2105–2114. https://doi.org/10.1046/j.0953-816x.2001.01591.x

International Association for the Study of Pain Home Page. Available online: https://www.iasp-pain.org/GlobalYear/NeuropathicPain (accessed on 26 October 2020)

Isbrucker RA, Burdock GA (2006) Risk and safety assessment on the consumption of licorice root (Glycyrrhiza sp.), its extract and powder as a food ingredient, with emphasis on the pharmacology and toxicology of glycyrrhizin. Regul Toxicol Pharmacol 46:167–192. https://doi.org/10.1016/j.yrtph.2006.06.002

Ito M, Ono K, Hitomi S, Nodai T, Sago T, Yamaguchi K, Harano N, Gunnjigake K, Hosokawa R, Kawamoto T, Inenaga K (2017) Prostanoid-dependent spontaneous pain and PAR(2)-dependent mechanical allodynia following oral mucosal trauma: involvement of TRPV1, TRPA1 and TRPV4. Mol Pain 13:1744806917704138. https://doi.org/10.1177/1744806917704138

Kawakami Z, Ikarashi Y, Kase Y (2011) Isoliquiritigenin is a novel NMDA receptor antagonist in kampo medicine yokukansan. Cell Mol Neurobiol 31:1203–1212. https://doi.org/10.1007/s10571-011-9722-1

Kim JY, Park SJ, Yun KJ, Cho YW, Park HJ, Lee KT (2008) Isoliquiritigenin isolated from the roots of Glycyrrhiza uralensis inhibits LPS-induced iNOS and COX-2 expression via the attenuation of NF-kappaB in RAW 264.7 macrophages. Eur J Pharmacol 14:175–184. https://doi.org/10.1016/j.ejphar.2008.01.032

Kono T, Satomi M, Chisato N, Ebisawa Y, Suno M, Asama T, Karasaki H, Matsubara K, Furukawa H (2010) Topical application of hangeshashinto (TJ-14) in the treatment of chemotherapy-induced Oral Mucositis. World J Oncol 1:232–235. https://doi.org/10.4021/wjon263w

Kono T, Kaneko A, Matsumoto C, Miyagi C, Ohbuchi K, Mizuhara Y, Miyano K, Uezono Y (2014) Multitargeted effects of hangeshashinto for treatment of chemotherapy-induced oral mucositis on inducible prostaglandin E2 production in human oral keratinocytes. Integr Cancer Ther 13:435–445. https://doi.org/10.1177/1534735413520035

Kovalsky Y, Amir R, Devor M (2009) Simulation in sensory neurons reveals a key role for delayed Na+ current in subthreshold oscillations and ectopic discharge: implications for neuropathic pain. J Neurophysiol 102:1430–1442. https://doi.org/10.1152/jn.00005.2009

Liang J, Liu X, Zheng J, Yu S (2013a) Effect of amitriptyline on tetrodotoxin-resistant Nav1.9 currents in nociceptive trigeminal neurons. Mol Pain 22(9):31. https://doi.org/10.1186/1744-8069-9-31

Liang L, Fan L, Tao B, Yaster M, Tao YX (2013b) Protein kinase B/Akt is required for complete Freund's adjuvant-induced upregulation of Nav1.7 and Nav1.8 in primary sensory neurons. J Pain 14:638–647. https://doi.org/10.1016/j.jpain.2013.01.778

Lindenlaub T, Sommer C (2000) Partial sciatic nerve transection as a model of neuropathic pain: a qualitative and quantitative neuropathological study. Pain. 15:97–106. https://doi.org/10.1016/S0304-3959(00)00354-7

Matsuda C, Munemoto Y, Mishima H, Nagata N, Oshiro M, Kataoka M, Sakamoto J, Aoyama T, Morita S, Kono T (2015) Double-blind, placebo-controlled, randomized phase II study of TJ-14 (Hangeshashinto) for infusional fluorinated-pyrimidine-based colorectal cancer chemotherapy-induced oral mucositis. Cancer Chemother Pharmacol 76:97–103. https://doi.org/10.1007/s00280-015-2767-y

Messier C, Epifano F, Genovese S, Grenier D (2012) Licorice and its potential beneficial effects in common oro-dental diseases. Oral Dis 18:32–39. https://doi.org/10.1111/j.1601-0825.2011.01842.x

Moghadamnia AA, Motallebnejad M, Khanian M (2009) The efficacy of the bioadhesive patches containing licorice extract in the management of recurrent aphthous stomatitis. Phytother Res 23:246–250. https://doi.org/10.1002/ptr.2601

Moriello AS, Luongo L, Guida F, Christodoulou MS, Perdicchia D, Maione S, Passarella D, Marzo VD, Petrocellis L (2016) Chalcone derivatives activate and desensitize the transient receptor potential ankyrin 1 cation channel, subfamily A, member 1 TRPA1 ion channel: structure-activity relationships in vitro and anti-nociceptive and anti-inflammatory activity in vivo. CNS Neurol Disord Drug Targets 15:987–994. https://doi.org/10.2174/1871527315666160413123621

Na AY, Yang EJ, Jeon JM, Ki SH, Song KS, Lee S (2018) Protective effect of isoliquiritigenin against ethanol-induced hepatic steatosis by regulating the SIRT1-AMPK pathway. Toxicol Res 34:23–29. https://doi.org/10.5487/TR.2018.34.1.023

Nakamura T, Miyoshi N, Ishii T, Nishikawa M, Ikushiro S, Watanabe T (2016) Activation of transient receptor potential ankyrin 1 by quercetin and its analogs. Biosci Biotechnol Biochem 80:949–954. https://doi.org/10.1080/09168451.2015.1132148

Nodai T, Hitomi S, Ono K, Masaki C, Harano N, Morii A, Sago-Ito M, Ujihara I, Hibino T, Terawaki K, Omiya Y, Hosokawa R, Inenaga K (2018) Endothelin-1 elicits TRP-mediated pain in an acid-induced oral ulcer model. J Dent Res 97:901–908. https://doi.org/10.1177/0022034518762381

Noguchi C, Yang J, Sakamoto K, Maeda R, Takahashi K, Takasugi H, Ono T, Murakawa M, Kimura J (2008) Inhibitory effects of isoliquiritigenin and licorice extract on voltage-dependent K^+ currents in H9c2 cells. J Pharmacol Sci 108:439–445. https://doi.org/10.1254/jphs.08227FP

Peng F, Du Q, Peng C, Wang N, Tang H, Xie X, Shen J, Chen J (2015) A review: the pharmacology of isoliquiritigenin. Phytother Res 29:969–977. https://doi.org/10.1002/ptr.5348

Revers FE (1956) Clinical and pharmacological investigations on extract of licorice. Acta Med Scand Suppl 312:749–751. https://doi.org/10.1111/j.0954-6820.1956.tb17084.x

Shao CJ, Gao Y, Zhao L, Jin D, Wang D, Wang DQ (2015) Co-application of lidocaine and QX-572 induces divergent pain behaviours in mice. J Pharm Pharmacol 67:1272–1278. https://doi.org/10.1111/jphp.12419

Shi Y, Wu D, Sun Z, Yang J, Chai H, Tang L, Guo Y (2012) Analgesic and uterine relaxant effects of isoliquiritigenin, a flavone from Glycyrrhiza glabra. Phytother Res 26:1410–1417. https://doi.org/10.1002/ptr.3715

Shibata S (2000) A drug over the millennia: pharmacognosy, chemistry, and pharmacology of licorice. Yakugaku Zasshi 120:849–862. https://doi.org/10.1248/yakushi1947.120.10_849

Takahashi T, Takasuka N, Iigo M, Baba M, Nishino H, Tsuda H, Okuyama T (2004) Isoliquiritigenin, a flavonoid from licorice, reduces prostaglandin E2 and nitric oxide, causes apoptosis, and

suppresses aberrant crypt foci development. Cancer Sci 95:448–453. https://doi.org/10.1111/j.1349-7006.2004.tb03230.x

Takayama Y, Uta D, Furue H, Tominaga M (2015) Pain-enhancing mechanism through interaction between TRPV1 and anoctamin 1 in sensory neurons. Proc Natl Acad Sci U S A 21:5213–5218. https://doi.org/10.1073/pnas.1421507112

Tibbs GR, Posson DJ, Goldstein PA (2016) Voltage-gated ion channels in the PNS: novel therapies for neuropathic pain? Trends Pharmacol Sci 37:522–542. https://doi.org/10.1016/j.tips.2016.05.002

Yamaguchi K, Ono K, Hitomi S, Ito M, Nodai T, Goto T, Harano N, Watanabe S, Inoue H, Miyano K, Uezono Y, Matoba M, Inenaga K (2016) Distinct TRPV1- and TRPA1-based mechanisms underlying enhancement of oral ulcerative mucositis-induced pain by 5-fluorouracil. Pain. 157:1004–1020. https://doi.org/10.1097/j.pain.0000000000000498

Yamashita T, Araki K, Tomifuji M, Kamide D, Tanaka Y, Shiotani A (2015) A traditional Japanese medicine–Hangeshashinto (TJ-14)—alleviates chemoradiation-induced mucositis and improves rates of treatment completion. Support Care Cancer 23:29–35. https://doi.org/10.1007/s00520-014-2315-z

Yang R, Wang LQ, Yuan BC, Liu Y (2015) The pharmacological activities of licorice. Planta Med 81:1654–1669. https://doi.org/10.1055/s-0035-1557893

Zhao P, Lieu T, Barlow N, Metcalf M, Veldhuis NA, Jensen DD, Kocan M, Sostegni S, Haerteis S, Baraznenok V, Henderson I, Lindström E, Guerrero-Alba R, Valdez-Morales EE, Liedtke W, McIntyre P, Vanner SJ, Korbmacher C, Bunnett NW (2014) Cathepsin S causes inflammatory pain via biased agonism of PAR2 and TRPV4. J Biol Chem 26:27215–27234. https://doi.org/10.1074/jbc.M114.599712

Zhu G, Ma S, Li X, Zhang P, Tang L, Cao L, Liu A, Sugita T, Tomoda T (2018) The effect of ethanol extract of Glycyrrhiza uralensis on the voltage-gated sodium channel subtype 1.4. J Pharmacol Sci 136:57–65. https://doi.org/10.1016/j.jphs.2017.11.008

Zimmermann M (1983) Ethical guidelines for investigations of experimental pain in conscious animals. Pain. 16:109–110. https://doi.org/10.1016/0304-3959(83)90201-4